Halogen…π Interactions in the Complexes of Fluorenonophane With Haloforms

Svitlana V. Shishkina (sveta@xray.isc.kharkov.com)
SSI "Institute for Single Crystals" https://orcid.org/0000-0002-3946-1061
Viktoriya V. Dyakonenko
SSI "INstitute for Single Crystals" NAS of Ukraine
Oleg V. Shishkin
SSI "Institute for Single Crystals" NAS of Ukraine
Volodimir P. Semynozhenko
SSI Institute for Single Crystals NAS of Ukraine: Naukovo-tehnologicnij kompleks Institut monokristaliv Nacional'na akademia nauk Ukraini
Tatiana Yu. Bogashchenko
A.V.Bogatsky Physico-Chemical Institute NAS of Ukraine
Alexander Yu. Lyapunov
A.V.Bogatsky Physico-Chemical Institute NAS of Ukraine
Tatiana I. Kirichenko
A.V.Bogatsky Physico-Chemical Institute NAS of Ukraine

Research Article

Keywords: Molecular crystals, Intermolecular interactions, Halogen bonds, Quantum-chemical calculations

Posted Date: July 30th, 2021

DOI: https://doi.org/10.21203/rs.3.rs-747526/v1

Version of Record: A version of this preprint was published at Structural Chemistry on October 19th, 2021. See the published version at https://doi.org/10.1007/s11224-021-01839-2.

Abstract

The study of two complexes of fluorenonophane with $CHCl_3$ and $CHBr_3$ molecules has revealed that they differ mainly by the halogen bonds between host and guest molecules. The experimental and theoretical quantum chemical study has shown that the strength of a halogen bond depends on the nature of a halogen atom as well as its orientation to the π-system. The more positive electrostatic potential was revealed at the bromine atom indicating the stronger halogen bond with its participation that was confirmed by the interaction energies calculated for corresponding dimers and the evaluation of the true energy of a halogen bond. The orientation of the chlorine atom at the carbon aromatic atom instead of the center of the benzene ring leads to the shortest Hal…C distance that points out the stronger interaction according to the geometrical characteristics. The EDA analysis of the fluorenonophane complexes with $CHCl_3$ and $CHBr_3$ and their analogs with one halogen atom replaced by the hydrogen atom allows us to presume that the nature of halogen bonding is rather dispersive than electrostatic.

Introduction

Weak intermolecular interactions of various types are of great interest for many years [1-4]. Special attention is paid to interactions called halogen bonds [5, 6]. It was demonstrated that halogen atoms in inorganic and organic halides can form complexes with molecules containing heteroatoms with lone pairs, for example, oxygen and nitrogen [7, 8]. At first, such interactions were found in the crystal phase [9], but evidence of their existence in a solution [10, 11] and even in a gas phase [12, 13] was also presented. The further study of halogen bonds has shown that these interactions are important for the formation of supramolecular complexes [14-16], protein-ligand interactions [17-22], crystal structures [23, 24].

As recommended by IUPAC, a halogen bond can be defined as "…an attractive interaction between an electrophilic region associated with a halogen atom in a molecular entity and a nucleophilic region in another or the same, molecular entity" [25]. Halogen bonds are described in the same way as hydrogen bonds. Exactly, a halogen bond is denoted by the three dots in R–X…Y, where R–X (X = Cl, Br, I) is the halogen bond donor with an electron-poor region and Y is the halogen bond acceptor containing an electron-rich region. Such a definition is based on the theoretical analysis of halogen bonding. A positive electrostatic potential region has to be located on the outermost portion of the halogen's surface centered on the R–X axis and was named "σ-hole" [26-28]. The strong directionality and electrostatic character of halogen bonding were expected [25, 29, 30], but a more detailed study of the nature of this interaction resulted in the conclusion that halogen bonds depend more strongly on the contributions from dispersion forces [31, 32].

The next question concerns the interaction strength of halogen bonding. The strength of a classical hydrogen bond can be evaluated from the characteristics of a (3,-1) bond critical point determined within Bader's theory "Atoms in molecules" between a hydrogen atom and a proton acceptor atom [33]. According to Espinosa's correlated equation, the potential energy in a (3,-1) bond critical point correlates

with the hydrogen bond energy [34]. However, the application of this equation to weak interactions like halogen bonds is very questionable. Another way to estimate the strength of intermolecular interactions is by studying their role in crystal packing formation [35]. Such a method was applied for the analysis of intermolecular interactions in crystals of the simplest halomethanes [36-38] where halogen bonds were expected to be the strongest interactions. However, the role of halogen bonds in crystal structure formation proved to be smaller than the role of non-specific interactions indicating the weak character of these interactions.

Despite their low strength, weak intermolecular interactions are quite effective in the formation of host-guest complexes [39-41]. The search for new efficient host molecules for molecular complexes led us to the synthesis (Scheme 1) of the fluorenonophane **3** representing a new group of macrocyclic receptors for organic molecules. Earlier, it was demonstrated that such types of hosts have a hollow intramolecular cavity limited by two fluorenone and two phenylene fragments [42]. Geometric parameters of the cavity allow different organic molecules, especially aromatic and heteroaromatic molecules, to settle easily within this cavity forming stable molecular complexes. The main intermolecular interaction that stabilizes complexes of such a type is the stacking between electron-rich fragments.

In this paper, we present the complexes of fluorenonophane **3** with the chloroform (**3Cl**) and bromoform (**3Br**). The halogen….π interactions are expected to be the strongest in these complexes providing their existence.

Experimental part.

Synthesis

Dibromide 1 was prepared according to the literature procedure [43], hydroquinone monobenzoate is commercially available and was used without further purification. Anhydrous acetonitrile and DMF were distilled from calcium hydride, other solvents were used as received. Column chromatography purification was performed with Silica gel 60 (Merck, 0.063–0.100 mm). Thin-layer chromatography (TLC) was performed on Merck pre-coated plates (silica gel 60 F_{254}). The plates were inspected by fluorescence quenching under UV light or, if required, developed in I_2 vapor. ^{1}H NMR spectra were recorded with a Varian VXR-300 spectrometer at 300 MHz with DMSO-d_6 as a solvent. Chemical shifts were reported in ppm downfield from internal Me_4Si. Electron impact mass spectra were obtained from an MX-1321 mass spectrometer with direct sample admission into the ion source operating at 70 eV.

Bisphenol 2. Dibromide **1** (3.66 g, 10 mmol) and hydroquinone monobenzoate (5.14 g, 24 mmol) were added to a suspension of K_2CO_3 (9.96 g, 72 mmol) in dry MeCN (200 mL) under an argon atmosphere. The suspension was stirred vigorously and heated under reflux for 15 h. After cooling down to room temperature, the suspension was filtered and the solvent was removed in vacuo. The residue was washed with diluted HCl (1:10) (50 mL), H_2O (50 mL), and hot MeOH (30 mL). The crude bisbenzoate was added to a solution of KOH (2.72 g, 49 mmol) in H_2O (27 mL) and EtOH (523 mL). The reaction mixture was

refluxed then for 6.5 h. After cooling down to room temperature, the solvent was removed in vacuo, diluted HCl (1:10) was added to the residue to adjust the pH of the aqueous layer to 5 and the crude bisphenol was extracted with $CHCl_3$ (4´100 mL). The organic phase was washed with saturated aqueous $NaHCO_3$ (2´200 mL), H_2O (200 mL), and saturated aqueous NaCl (200 mL) and then dried ($MgSO_4$). The solvent was removed in vacuo to afford **2** as a yellow solid (2.33 g, 55%): mp > 250°C dec. EIMS 424 (M^+); ^1H NMR δ 5.00 (s, 4H), 6.65 (d, *J* = 8.7 Hz, 4H), 6.79 (d, *J* = 9.0 Hz, 4H), 7.57–7.64 (m, 4H), 7.71 (d, *J* = 8.4 Hz, 2H), 8.80 (s, 2H). Anal. Calcd. for $C_{27}H_{20}O_5$: C, 76.40; H, 4.75. Found: C, 76.27; H, 4.99.

Cyclophane 3. A solution of **1** (732 mg, 2 mmol) and **2** (848 mg, 2 mmol) in dry degassed DMF (60 mL) was added dropwise over 10 h to a stirred suspension of K_2CO_3 (1.656 g, 12 mmol) in DMF (140 mL) under argon at 80°C and the reaction mixture was then heated and stirred for further 45 h. After being cooled down to room temperature, the suspension was filtered off, the solid was washed with DMF (2´20 mL), and the solvent was removed in vacuo. The residue was partitioned between $CHCl_3$ (300 mL) and aqueous 5% NaOH (70 mL). The organic phase was washed with H_2O (100 mL) and saturated aqueous NaCl (100 mL) and then dried ($MgSO_4$). Evaporation of the solvent afforded a residue which was subjected to column chromatography ($CHCl_3$/MeOH, 100:1) to yield **3** as a light-yellow solid (188 mg, 15%): mp > 250°C dec. EIMS 628 (M^+); ^1H NMR δ5.15 (s, 8H), 6.71 (s, 8H), 7.44 (s, 4H), 7.55 (s, 8H). Anal. Calcd. for $C_{42}H_{28}O_6$: C, 80.24; H, 4.49. Found: C, 80.38; H, 4.63.

X-ray diffraction study.

The crystals of **3Cl** ($C_{42}H_{28}O_6 \bullet 2CCl_3$) are triclinic, space group P. At 100 K ***a*** = 9.163(2) Å, ***b*** = 10.802(3) Å, ***c*** = 11.757(4) Å, a = 113.59(3)°, b = 95.10(3)°, g = 112.77(2)°, V = 941.5(5) $Å^3$, d_{calc} = 1.530 g/cm, Z = 1, m = 0.509 mm^{-1}. Intensities of 23762 reflections (5472 unique reflections, R_{int} = 0.025) were measured using an “Xcalibur-3” diffractometer (graphite-monochromated MoK_a radiation, w-scan, a CCD detector, $2q_{max}$ = 60°). Absorption corrections were performed using the multi-scans method (T_{min} = 0.898, T_{max} = 0.971).

The crystals of **3Br** ($C_{42}H_{28}O_6 \bullet 2CBr_3$) are monoclinic, space group $P2_1/n$. At 100 K ***a*** = 10.9417(2) Å, ***b*** = 12.4492(2) Å, ***c*** = 14.4471(3) Å, b = 90.933(2)°, V = 1967.66(6) $Å^3$, d_{calc} = 1.914 g/cm, Z = 2, m = 6.172 mm^{-1}. Intensities of 8506 reflections (4401 unique reflections, R_{int} = 0.029) were measured using an “Xcalibur-3” diffractometer (graphite-monochromated MoK_a radiation, w-scan, a CCD detector, $2q_{max}$ = 55°). Absorption corrections were performed using the multi-scans method (T_{min} = 0.468, T_{max} = 0.732).

The structures were solved by the direct method using the SHELXTL program package [44, 45] implemented in the OLEX2 program [46]. Positions of the hydrogen atoms were located from electron density difference maps and refined by the “riding” model with $U_{iso} = 1.2U_{eq}$ of the carrier atom. Full-matrix least-squares refinement of the structures against F^2 in anisotropic approximation for non-hydrogen atoms using 5472 (**3Cl**), 4401 (**3Br**) reflections was converged to: wR_2 = 0.049 (R_1 = 0.035 for 4141 reflections with F>4σ(F), S = 1.092) for structure **3Cl** and wR_2 = 0.073 (R_1 = 0.036 for 2684

reflections with F>4σ(F), S = 0.917) for structure **3Br**. The final atomic coordinates and crystallographic data for **3Cl** and **3Br** have been deposited with the Cambridge Crystallographic Data Centre, 12 Union Road, CB2 1EZ, UK (fax: +44-1223-336033; e-mail: deposit@ccdc.cam.ac.uk) and are available on request quoting the deposition numbers CCDC 647971 for **3Cl** and CCDC 2098245 for **3Br**.

Analysis of crystal structures from the energetic viewpoint.

Crystal structure analysis was performed within the approach based on quantum chemical calculations of pairwise interaction energies between molecules in a crystal [47]. Any molecule in a crystal may be considered as a basic unit of a crystal packing (BU_0), and its first coordination sphere can be constructed using the standard procedure within the Mercury program [48]. This option allows us to determine all molecules for which the distance between atoms of the basic BU_0 and its symmetrical equivalents is shorter than van der Waals radii sum plus 1 Å at least for one pair of atoms. In the case of Z' > 1, this procedure should be applied to each of the molecules found in the asymmetric part of the unit cell. The selected fragment of the crystal packing can be divided into dimers where one molecule is basic and the other one belongs to its first coordination sphere. The molecular geometries of these dimers were not optimized. Taking into account the well-known effect of X–H bonds shortening in the X-ray diffraction study [49], the positions of hydrogen atoms were normalized to 1.089 Å for C–H and 0.993 Å for O–H bonds, according to neutron diffraction data [50]. The pairwise interaction energies were calculated using the B97D3 density functional method [51] with the def2-TZVP basis set [52, 53] and corrected for a basis set superposition error by the counterpoise method [54]. All single-point calculations were performed within the Gaussian03 software [55].

The energy-vector diagrams (EVD) were proposed for the graphic representation of the obtained data [56]. The calculated interaction energy between two molecules takes on vector properties if it originates from the geometrical center of the basic BU_0 and is directed toward the geometrical center of a symmetrically equivalent BU_i. The use of such an assumption makes it possible to visualize the interaction energies in a crystal as a set of such vectors (L_i) originating from the geometrical center of the basic BU. The length of each energy vector L_i is calculated using the following equation:

$$L_i = \frac{R_i E_i}{2E_{str}} \qquad (1)$$

where R_i is the distance between the geometrical centers of the interacted building units BU_0-BU_i, E_i is their interaction energies, and E_{str} is the strongest pairwise interaction energy in the crystal.

The energy-vector diagram represents the image of a molecule in terms of the strength and directionality of its intermolecular interactions in a crystal. Replacing the basic molecule with such a vector image and applying all symmetry operations to it result in the visualization of a crystal packing in terms of interaction energies between molecules. This method allows us to define the most strongly bound

fragments of a crystal packing such as a primary basic structural motif (BSM_1) or a secondary basic structural motif (BSM_2) [57].

Analysis of the interaction energy

The estimation of the true energy of halogen bonding

To evaluate the true energy of halogen bonding the approach proposed earlier [58] was used. The difference in intermolecular interaction energies for halogen bonded dimers and model dimers where the interacting halogen is replaced by the hydrogen atom may be used as the approximate (within 0.1÷0.2 kcal/mol) true energy of a halogen bond.

Decomposition of the Interaction Energy

The contribution of all types of interactions to the total interaction energy was studied using the modified method of Morokuma and Kitaura [59] namely Localized Molecular Orbital Energy Decomposition Analysis (LMOEDA) [60] implemented in the GAMESS-US software package [61]. For these calculations, we used the geometry of molecule pairs extracted from the experimental data. The calculations of interaction energies were carried out using the m06-2x method [62] and the 6-311G(d,p) basis set [63] and corrected for a basis set superposition error by the counterpoise method. The accuracy of the DFT grid [64] was increased to ultrafine (99 radial shells with 590 Lebedev points in each). Pulay's direct inversion of the iterative subspace (DIIS) interpolation [65, 66] was used in these calculations to increase the convergence speed.

Results And Discussion

Single crystals of complexes of the fluorenonophane **3** with the chloroform (**3Cl**) and bromoform (**3Br**) suitable for X-ray crystallography were obtained by slow evaporation of their solutions in the corresponding haloform. X-ray diffraction study reveals the 1:2 (**3**/haloform) stoichiometry of these complexes. In the crystal phase, both complexes are situated in a special position in the inversion center located at the geometrical center of the macrocycle (Fig. 1). Therefore, the average planes of both fluorenone and phenylene fragments are strictly parallel. Carbonyl groups of the fluorenone fragments are oriented in opposite directions (anti-orientation).

The molecules of haloform occupy the boundary part of the macrocyclic cavity (Fig. 1) and are bonded with the fluorenone fragment by the C–H…O=C hydrogen bonds (the H…O distances and C–H…O angles are 2.29 Å, 141^o in **3Cl** and 2.48 Å, 130^o in **3Br**, respectively).

In addition, an interaction between one of the halogen atoms of a haloform molecule and the π-system of the benzene ring is found in the complexes **3Cl** and **3Br**. In the case of the **3Cl** complex, the C–Cl bond is inclined to the aromatic ring (the C–Cl…X angle is 154.7^o, where the X is a centroid of the benzene ring). Inspection of the Cl…C(Ar) distances reveals that the chlorine atom is shifted to one of the aromatic

carbon atoms. The shortest Cl…C(Ar) distance is 3.39 Å that is significantly smaller than their van der Waals radii sum [67] (3.61 Å) and the value of the C–Cl…C(Ar) angle is 177.3(5)°. This indicates a presence of strong enough specific interactions between the chlorine atom and one aromatic carbon atom.

In the case of **3Br**, the shortest Br…C distance (3.80 Å) is longer than the corresponding van der Waals radii sum (3.68 Å). However, the C–Br bond is oriented exactly towards the center X of the benzene ring. The Br…X distance (3.65 Å) is shorter than any Br…C(Ar) distance and is slightly smaller than the van der Waals radii sum of carbon and bromine atoms. The C–Br…X angle (173.4°) is close to 180° which is in agreement with the previous findings for halogen bonds [5, 6]. This indicates the existence of halogen bonding between the bromine atom and the whole π-system of the aromatic ring.

The electrostatic potential for chloroform and bromoform was calculated using the B3LYP/6-311G(d,p) method. It has been revealed that the area of the positive electrostatic potential at the halogen atom is oriented to the aromatic carbon atom in complex **3Cl** or to the center of the benzene ring in **3Br** (Fig. 2). The highest positive potential is 0.054 eV at the chlorine atom and 0.082 eV at the bromine atom participating in the halogen bonds with π-system in the complexes **3Cl** and **3Br**.

Additional evidence of the Hal…π interactions in the complexes **3Cl** and **3Br** can be obtained from the results of the AIM analysis (Fig. 3). The existence of (3,-1) bond critical points and bond paths indicates the interactions between a halogen atom and one of the carbon aromatic atoms. Unfortunately, the characteristics of these bond critical points do not allow comparing the strength of the halogen bonds.

One of the modern methods allowing to compare intermolecular interactions in similar complexes or structures is the Hirshfeld surface analysis [69] that can be performed using the CrystalExplorer program [70]. Such an analysis has revealed the brightest red spots on the d_{norm}-mapped Hirshfeld surfaces of the complexes **3Cl** and **3Br** in the area of the carbonyl oxygen atoms (Fig. 4). This indicates the existence of C–H…O short contacts in both complexes. A very small red area is observed at one of the chlorine atoms in the complex **3Cl** indicating its participation in a halogen bond while any red area is found at a bromine atom in the complex **3Br**. The results of the analysis of Hirshfeld surfaces showed that halogen bonds in the studied structures are weak enough and can hardly cause the formation of these ‘host-guest” complexes.

The evaluation of the contributions of short contacts of different types to the total Hirshfeld surface (Fig. 5) has shown that the contribution of H…Hal/Hal…H contacts is higher in the complex **3Cl** while the C…Hal/Hal…C contacts contribution is higher in the complex **3Br**. It may be concluded from these data that the bromine atom forms the stronger halogen bonds as an electrophilic entity and weaker interactions as a proton acceptor. This conclusion corresponds completely with the theoretical conception of halogen bonding but does not coincide with the results of the geometrical characteristics analysis of intermolecular interactions in the complexes **3Cl** and **3Br**.

Analysis of pairwise interaction energies in a crystal proposed by Prof. Shishkin [47, 57] proved to be more informative taking into account both specific and non-specific interactions. Such an analysis performed for the crystal structures of **3Cl** and **3Br** has revealed that the strongest interactions are stacking between neighboring fluorenonophane molecules and interactions between host and guest molecules (Table 1). These strong interactions result in the formation of a column due to stacking interactions where each fluorenonophane molecule is bound with two haloform molecules (Fig. 6).

The main difference observed due to the analysis of pairwise interaction energies in the structures of **3Cl** and **3Br** is the energy ratio between stacking dimers and host-guest dimers (Table 1). The dimer formed by stacking interactions proved to have the highest interaction energy in the crystals of **3Cl** while the dimer formed due to the C–H…O hydrogen bond, C–Br…π halogen bond, and non-specific interactions has the highest energy in the crystals of **3Br** (Fig. 6).

Taking into account that these structural motifs differ mainly by the nature of a halogen atom, the contribution of the halogen bond energy into total interaction energy in the host-guest dimer should be evaluated. The simplest way to do it is the application of the approach proposed earlier [58]. According to this approach, a simple substitution scheme of a halogen atom by a hydrogen atom can be used. The energy of halogen bonding is considered as a difference in energy between the dimer containing a halogen-substituted moiety and the dimer containing the same moiety with a hydrogen atom instead of a halogen. The application of this approach to the complexes **3Cl** and **3Br** allows us to evaluate the true energy of the halogen bonds as -3.87 kcal/mol in the complex **3Cl** and -4.94 kcal/mol in the complex **3Br**. It should be noted that such an approach does not give any information about the nature of halogen bonding.

To understand the nature of halogen bonding, the energy decomposition analysis (EDA) was carried out for dimers formed by fluorenonophane and a haloform molecule and the same dimers with a halogen atom replaced by a hydrogen atom. The results of this analysis clearly showed that the dispersion component of the total interaction energy underwent the most significant change (Table 2). The change in the electrostatic component is much smaller. Therefore, we can conclude that halogen bonding should be associated rather with dispersion forces than with electrostatic interactions.

Conclusions

The thorough study of two complexes of fluorenonophane with haloform molecules indicated the C–Cl…π and C–Br…π halogen bonds as the main difference in their structures. At that, the halogen bonding strength depends on the nature of a halogen atom and its orientation to the aromatic ring. The analysis of geometrical characteristics as well as the Hirshfeld surface analysis proved to be uninformative for comparing halogen bonds formed by chlorine or bromine atoms. The analysis of electrostatic potential at the halogen atoms participating in halogen bonds has revealed the highest positive potential at the bromine atom. The study of the halogen bonding role in the complex formation using the analysis of interaction energies in the corresponding dimers also showed the stronger halogen…π bond formed by

the bromine atom. The energy decomposition analysis has revealed that the nature of halogen bonding is rather dispersive than electrostatic.

Declarations

Funding

The authors thank the National Academy of Sciences of Ukraine for financial support in the frame of the projects “New supramolecular systems based on cyclophanes with fluorenone and benzimidazole fragments. Design, synthesis, structure, perspectives" (0120U100122) and "Functional materials for biomedical purposes based on halogen-containing organic compounds" (0120U102660).

Conflict of interest

The authors declare no conflict of interest.

Availability of data and material

Experimental X-ray diffraction data are available from the Cambridge Crystallographic Data Centre on request quoting the deposition numbers CCDC 647971 for **3Cl** and CCDC 2098245 for **3Br**.

Code availability

Not applicable.

Authors' contributions

Optional

References

1. Hobza P, Zahradnik R (1980) Weak intermolecular interactions in chemistry and biology. Elsevier, Amsterdam, New York.
2. Dunitz JD (1996) Weak intermolecular interactions in solids and liquids. Molecular Crystals and Liquid Crystals Science and Technology. Section A. Molecular Crystals and Liquid Crystals 279:209–218.
3. Waller M, Grimme S (2015) Weak intermolecular interactions: a supermolecule approach. In: Leszczynski J. (eds) Handbook of Computational Chemistry, Springer, Dordrecht.
4. Maji R, Wheeler SE (2018) Chapter 10: Weak intermolecular interactions. 289–319. In: Tantillo DJ (eds) Applied Theoretical Organic Chemistry, World Scientific.
5. Metrangolo P, Resnati G (2015) Halogen bonding I. Springer, Impact on materials chemistry and life sciences. Springer.

6. Metrangolo P, Resnati G (2015) Halogen bonding II. Springer, Impact on materials chemistry and life sciences. Springer.
7. Mele A, Metrangolo P, Neukrich H, Pilati T, Resnati G (2005) A halogen-bonding-based heteroditopic receptor for alkali metal halides. J Am Chem Soc 127:14972–14973.
8. Metrangolo P, Neukrich H, Pilati T, Resnati G (2005) Halogen bonding based recognition processes: a world parallel to hydrogen bonding. Acc Chem Res 38:386–395.
9. Ouvrard C, Le Questel JY, Berthelot M, Laurence C (2003) Halogen-bond geometry: a crystallographic database investigation of dihalogen complexes. Acta Cryst B59:512–526.
10. Shishkin OV, Khrustalev VN, Lindeman SV, Ukhin Lyu, Orlova GI, Gribanova TN (1998) Structure of 5-nitro-2-tosylaminobenzaldehyde di(morpholin-4-yl)-aminal complex with carbon tetrachloride. Z Kristallogr 213:296–298.
11. Glaser R, Chen N, Wu H, Knotts N, Kaupp M (2004) ^{13}C NMR Study of Halogen Bonding of Haloarenes: Measurements of Solvent Effects and Theoretical Analysis. J Am Chem Soc 126:4412–4419.
12. Legon AC (1999) Angular and radial geometries, charge transfer and binding strength in isolated complexes B…ICl: some generalisations. Chem Phys Lett 314:472–480.
13. Legon AC (1999) Prereactive complexes of dihalogens XY with Lewis bases B in the gas phase: a systematic case for the halogen analogue B…XY of the hydrogen bond B…HX. Angew Chem, Int Ed 38:2686–2714.
14. Gildaay LC, Robinson SW, Barendt TA, Langton MJ, Mullaney BR, Beer PD (2015) Halogen bonding in supramolecular chemistry. Chem Rev 115:7118–7195.
15. Aackeröy CB, Hurley DP, Desper J (2012) Modulating supramolecular reactivity using covalent “switches” on a pyrazole platform. Cryst Growth Des 12:5806–5814.
16. Cavallo G, Metrangolo P, Milani R, Pilati T, Priimagi A, Resnati G, Terraneo G (2016) The halogen bond. Chem Rev 116:2478–2601.
17. Riley KE, Hobza P (2011) Strength and character of halogen bonds in protein-ligand complexes. Cryst Growth Des 11:4272–4278.
18. Parisini E, Metrangolo P, Pilati T, Resnati G, Terraneo G (2011) Halogen bonding in halocarbon-protein complexes: a structural survey. Chem Soc Rev 40:2267–2278.
19. Scholfield MR, Van der Zanden CM, Carter M, Ho PS (2013) Halogen bonding (X-Bonding): a biological perspective. Protein Sci 22:139–152.
20. Lu Y, Wang Y, Zhu W (2010) Nonbonding interactions of organic halogens in biological systems: implications for drug discovery and biomolecular design. Phys Chem Chem Phys 12:4543–4551.
21. Wilcken R, Zimmermann MO, Lange A, Joerger AC, Boeckler FM (2013) Principles and applications of halogen bonding in medicinal chemistry and chemical biology. J Med Chem 56:1363–1388.
22. Ho PS (2017) Halogen bonding in medicinal chemistry: from observation to prediction. Future Sci 9:637–640.

23. Aackeröy CB, Wijethunga TK, Desper J, Đaković M (2015) Crystal engineering with iodoethynylmitrobenzenes: a group of highly effective halogen bond donors. Cryst Growth Des 15:3853–3861.
24. Mukherjee A, Tothadi S, Desiraju GR (2014) Halogen bonds in crystal engineering: like hydrogen bonds yet different. Acc Chem Res 47:2514–2524.
25. Desiraju GR, Ho PS, Kloo L, Legon AC, Marquardt R, Metrangolo P, Politzer P, Resnati G, Rissanen K (2013) Definition of the halogen bond (IUPAC Recommendations 2013). Pure Appl Chem 85:1711–1713.
26. Politzer P, Lane P, Concha MC, Ma Y, Murray J.S (2007) An overview of halogen bonding. J Mol Model 13:305–311.
27. Politzer P, Murray JS, Clark T (2013) Halogen bonding and other σ-hole interactions: a perspective. Phys Chem Chem Phys 15:11178–11189.
28. Murray JS, Riley KE, Politzer P, Clark T (2010) Directional weak intermolecular interactions: σ-hole bonding. Aust J Chem 63:1598–1607.
29. Clark T, Hennemann M, Murray JS, Politzer P (2007) Halogen bonding: the σ-hole. J Mol Model 13:291–296.
30. Politzer P, Murray JS, Lane P (2007) σ-Hole bonding and hydrogen bonding: Competitive interactions. Int J of Quant Chem 107:3046–3052.
31. Riley KE, Hobza P (2008) Investigations into the nature of halogen bonding including symmetry adapted perturbation theory analyses. J Chem Theory Comput 4:232–242.
32. Kolář MH, Hobza P (2016) Computer modeling of halogen bonding and other σ-hole interactions. Chem Rev 116:5155–5187.
33. Bader RFW (1990) Atoms in molecules: a quantum theory. Oxford University Press, Oxford
34. Espinosa E, Molins E, Lecomte C (1998) Hydrogen bond strengths revealed by topological analyses of experimentally observed electron densities. Chem Phys Lett 285:170–173.
35. Shishkin OV, Zubatyuk RI, Shishkina SV, Dyakonenko VV, Medviediev VV (2014) Role of supramolecular synthons in the formation of the supramolecular architecture of molecular crystals revisited from an energetic viewpoint. Phys Chem Chem Phys 16: 6773–6786
36. Yufit DS, Zubatyuk R, Shishkin OV, Howard JAK (2012) Low- melting molecular complexes. Halogen bonds in molecular complexes of bromoform. Cryst Eng Comm 14:8222–8227
37. Yufit DS, Shishkin OV, Zubatyuk RI, Howard JAK (2014) Low- melting molecular complexes. Z Kristallogr 229:639–647
38. Yufit DS, Shishkin OV, Zubatyuk RI, Howard JAK (2014) Trimethyltrioxane (paraldehyde) and its halomethanes complexes: crystallization, structures, and analysis of packing motifs. Cryst Growth Des 14:4303–4309
39. Steed JW, Atwood JL (2009) Supramolecular Chemistry. Wiley, Chichester.

40. Lyapunov AYu, Kirichenko TI, Kulygina C, Zubatyuk R, Fonari M, Kyrychenko A, Doroshenko A (2015) New fluorenonocrownophanes containing azobenzene: synthesis, properties and interaction with paraquat. Journal of Inclusion Phenomena and Macrocyclic Chemistry 81:499–508.
41. Kikot LS, Kulygina CYu, Lyapunov AYu, Shishkina SV, Zubatyuk RI, Bogaschenko TYu, Kirichenko TI (2017) Complexation of molecular clips containing fragments of diphenylglycoluril and benzocrown ethers with paraquat and its derivatives. Beilstein Journal of Organic Chemistry 13:2056–2067.
42. Simonov YuA, Bogdashchenko TYu, Pastushok VN, Botoshanskii MM, Fonar' MS, Lyapunov AYu, Lukyanenko N G (2006) 2,6,8,12-Tetraoxa-4,10(1,4)-dibenzena-1,7(2,7)-difluorenacyclododecaphane-19,79-dione—A new macrocyclic receptor for polar organic molecules. Russ J Org Chem 42:1075–1082.
43. Haenel MW, Irngartinger H, Krieger C (1985) Transanulare wechselwirkung bei [m. n]phanen, 27. modelle für excimere und exciplexe: [2.2]phane des fluorens, 9-fluorenons und 9-fluorenyl-anions. Chem Ber 118:144–162.
44. Sheldrick GM (2015) SHELXT – integrated space-group and crystal-structure determination. Acta Cryst *A71*:3–8.
45. Sheldrick GM (2015) Crystal structure refinement with SHELXL. Acta Cryst C71:3–8.
46. Dolomanov OV, Bourhis LJ, Gildea RJ, Howard JAK, Puschmann H (2009) OLEX2: A complete structure solution, refinement and analysis program. J Appl Cryst 42:339–341.
47. Konovalova IS, Shishkina SV, Paponov BV, Shishkin OV (2010) Analysis of the crystal structure of two polymorphic modifications of 3,4-diamino-1,2,4-triazole based on the energy of the intermolecular interactions. CrystEngComm 12:909–916.
48. Macrae CF, Bruno IJ, Chisholm JA, Edgington PR, McCabe P, Pidcock E, Rodriguez-Monge L, Taylor R, van de Streek J, Wood PA (2008) Mercury CSD 2.0- new features for the visualization and investigation of crystal structures. J Appl Crystallogr 41:466–470.
49. Coppens P (1972) The use of a polarized hydrogen atom in X-ray structure refinement. Acta Crystallogr, Sect B: Struct Crystallogr Cryst Chem 28:1638–1640.
50. Allen FH, Bruno IJ (2010) Bond lengths in organic and metalorganic compounds revisited: X-H bond lengths from neutron diffraction data. Acta Crystallogr, Sect B: Struct Sci 66:380–386.
51. Grimme S, Ehrlich S, Goerigk L (2011) Effect of the damping function in dispersion corrected density functional theory. J Comput Chem 32:1456–1465.
52. Weigend F, Ahlrichs R (2005) Balanced basis sets of split valence, triple zeta valence and quadruple zeta valence quality for H to Rn: design and assessment of accuracy. Phys Chem Chem Phys 7:3297–3305.
53. Weigend F (2006) Accurate Coulomb-fitting basis sets for H to Rn. Phys Chem Chem Phys 8:1057–1065.
54. Boys SF, Bernardi F (1970) The calculation of small molecular interactions by the differences of separate total energies. Some procedures with reduced errors. Mol Phys 19:553–566.

55. Frisch MJ, Trucks GW, Schlegel HB, Scuseria GE, Robb MA, Cheeseman JR, Montgomery JA, Vreven T, Kudin KN, Burant JC, Millam JM, Iyengar SS, Tomasi J, Barone V, Mennucci B, Cossi M, Scalmani G, Rega N, Petersson GA, Nakatsuji H, Hada M, Ehara M, Toyota K, Fukuda R, Hasegawa J, Ishida M, Nakajima T, Honda Y, Kitao O, Nakai H, Klene M, Li X, Knox JE, Hratchian HP, Cross JB, Bakken V, Adamo C, Jaramillo J, Gomperts R, Stratmann RE, Yazyev O, Austin AJ, Cammi R, Pomelli C, Ochterski JW, Ayala PY, Morokuma K, Voth GA, Salvador P, Dannenberg JJ, Zakrzewski VG, Dapprich S, Daniels AD, Strain MC, Farkas O, Malick DK, Rabuck AD, Raghavachari K, Foresman JB, Ortiz JV, Cui Q, Baboul AG, Clifford S, Cioslowski J, Stefanov BB, Liu G, Liashenko A, Piskorz P, Komaromi I, Martin RL, Fox DJ, Keith T, Al-Laham MA, Peng CY, Nanayakkara A, Challacombe M, Gill PMW, Johnson B, Chen W, Wong MW, Gonzalez C, Pople JA (2004) Gaussian 03, Revision C 02; Gaussian, Inc: Wallingford CT.
56. Shishkin OV, Dyakonenko VV, Maleev AV (2012) Supramolecular architecture of crystals of fused hydrocarbons based on topology of intermolecular interactions. Cryst Eng Comm 14:1795–1804.
57. Shishkin OV, Zubatyuk RI, Shishkina SV, Dyakonenko VV, Medviediev VV (2014) Role of supramolecular synthons in the formation of the supramolecular architecture of molecular crystals revisited from an energetic viewpoint. Phys Chem Chem Phys 16:6773–6786.
58. Shishkin OV (2008) Evaluation of true energy of halogen bonding in the crystals of halogen derivatives of trityl alcohol. Chem Phys Lett 458:96–100.
59. Kitaura K, Morokuma K (1976) A new energy decomposition scheme for molecular interactions within the Hartree-Fock approximation. Int J Quantum Chem 10:325–340.
60. Su P, Li H (2009) Energy decomposition analysis of covalent bonds and intermolecular interactions. J Chem Phys 131:014102–1–15.
61. Schmidt MW, Baldridge KK, Boatz JA, Elbert ST, Gordon MS, Jensen JH, Koseki S, Matsunaga N, Nguyen KA, Su S, Windus TL, Dupuis M, Montgomery JrJA (1993) General atomic and molecular electronic structure system. J Comput Chem 14:1347–1363.
62. Zhao Y, Truhlar DG (2007) The M06 suite of density functionals for main group thermochemistry, thermochemical kinetics, noncovalent interactions, excited states, and transition elements: two new functionals and systematic testing of four M06-class functionals and 12 other functionals. Theor Chem Acc 120:215–241.
63. Raghavachari K, Binkley JS, Seeger R, Pople J A (1980) Self-consistent molecular orbital methods. 20. basis set for correlated wave-functions J Chem Phys72:650-654.
64. Lebedev VI, Laikov DN (1999) A quadrature formula for the sphere of the 131st algebraic order of accuracy. Dokl Mat 59:477–481.
65. Pulay P (1980) Convergence acceleration of iterative sequences. the case of SCF iteration. Chem Phys Lett 73:393–398.
66. Pulay P(1982) Improved SCF convergence acceleration. J Comput Chem 3:556–560.
67. Zefirov YuV, Zorky PM (1989) Van der Waals radii and their application in chemistry. Russ Chem Rev 58:421–441.

68. Sinnokrot MO, Sherrill CD (2004) Highly accurate coupled cluster potential energy curves for the benzene dimer: sandwich, t-shaped, and parallel-displaced configurations. J Phys Chem 108:10200–10207.
69. Spackman MA, Jayatilaka D (2009) Hirshfeld surface analysis. Cryst Eng Comm 11:19–32.
70. Turner MJ, McKinnon JJ, Wolff SK, Grimwood DJ, Spackman PR, Jayatilaka D, Spackman MA (2017) CrystalExplorer17. University of Western Australia.

Tables

Table 1. Symmetry codes, interaction energies of the basic unit with neighbors (E_{int}, kcal/mol) with the highest values (more than 5% of total interaction energy), and the contribution of this energy to the total interaction energy (%) in crystals of the complexes **3Cl** and **3Br** (for the full list of dimers see Tables S1).

Dimer	Symmetry operation	E_{int}, kcal/mol	The contribution to the total interaction energy, %	Type of interaction
Complex **3Cl**				
3Cl_d1	1+x,1+y,z	-17.00	9.4	stacking
3Cl_d2	-1+x,-1+y,z	-17.00	9.4	stacking
3Cl_d3	x,y,z	-13.89	7.7	C–H…O, C–Cl…π
3Cl_d4	1-x,1-y,1-z	-13.89	7.7	C–H…O, C–Cl…π
Complex **3Br**				
3Br_d1	x,y,z	-16.89	9.1	C–H…O, C–Br…π
3Br_d2	-x,1-y,-z	-16.89	9.1	C–H…O, C–Br…π
3Br_d3	1+x,y,z	-14.68	7.9	stacking
3Br_d4	-1+x,y,z	-14.68	7.9	stacking

Table 2. Components of the total interaction energy (in kcal/mol) calculated using the M06-2x/6-311G(d,p) method for the complexes **3Cl** and **3Br** and their analogs with a halogen replaced by a hydrogen atom (**3Cl/H** and **3Br/H**).

	3Cl	3Cl/H	3Br	3Br/H
Electrostatic energy (ES=)	-6.24	-5.05	-6.84	-5.84
Exchange energy (EX=)	-2.98	-2.07	-4.12	-3.81
Repulsion energy (REP=)	22.00	13.77	26.95	19.89
Polarization energy (POL=)	-3.96	-2.90	-3.62	-2.95
Dispersion energy (DISP=)	-22.06	-12.86	-27.35	-17.82
Total interaction energy (E=)	-13.24	-9.12	-14.97	-10.53

Figures

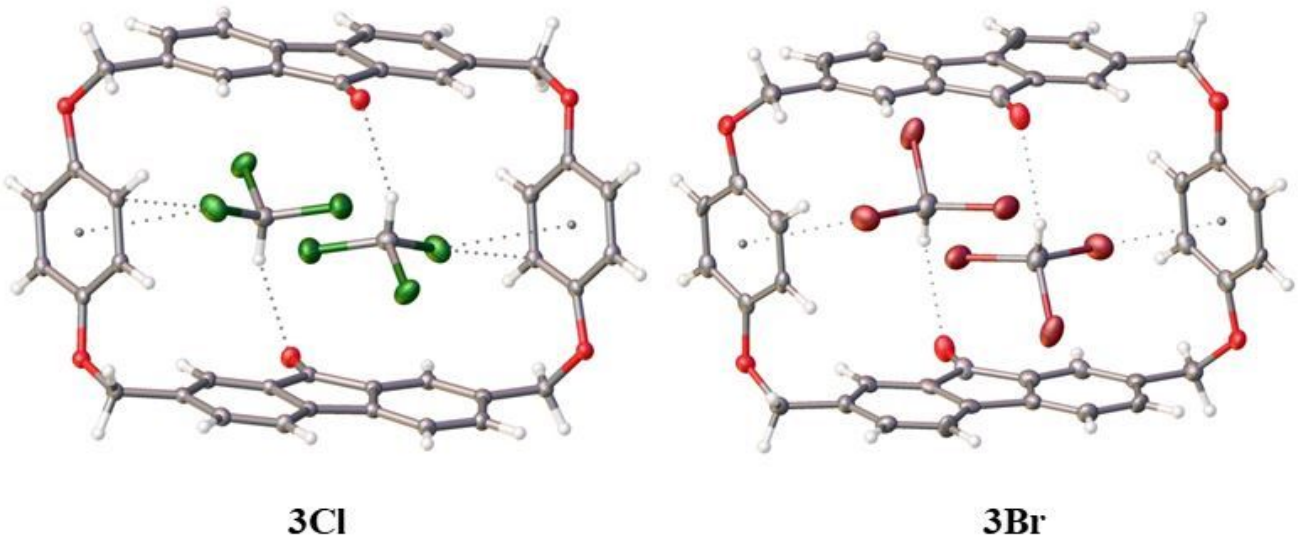

Figure 1

Structure of fluorenonophane complexes with chloroform (3Cl) and bromoform (3Br).

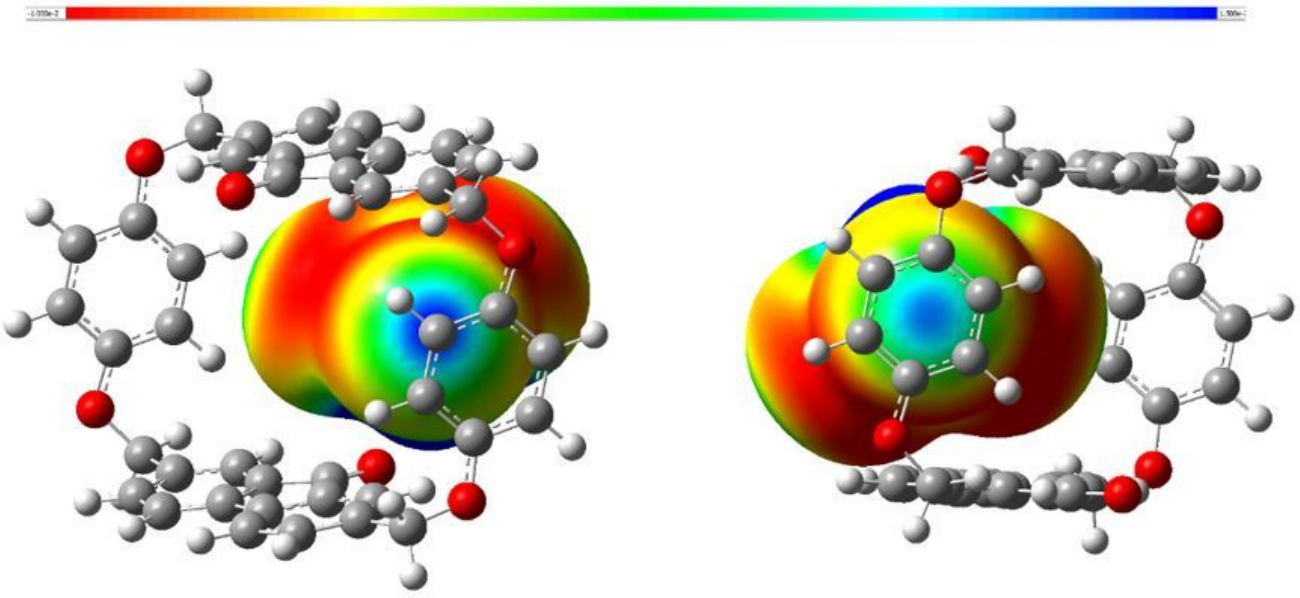

Figure 2

The electrostatic potential of a haloform molecule in the complexes 3Cl (on the left) and 3Br (on the right) calculated using the B3LYP/6-311G(d,p) method.

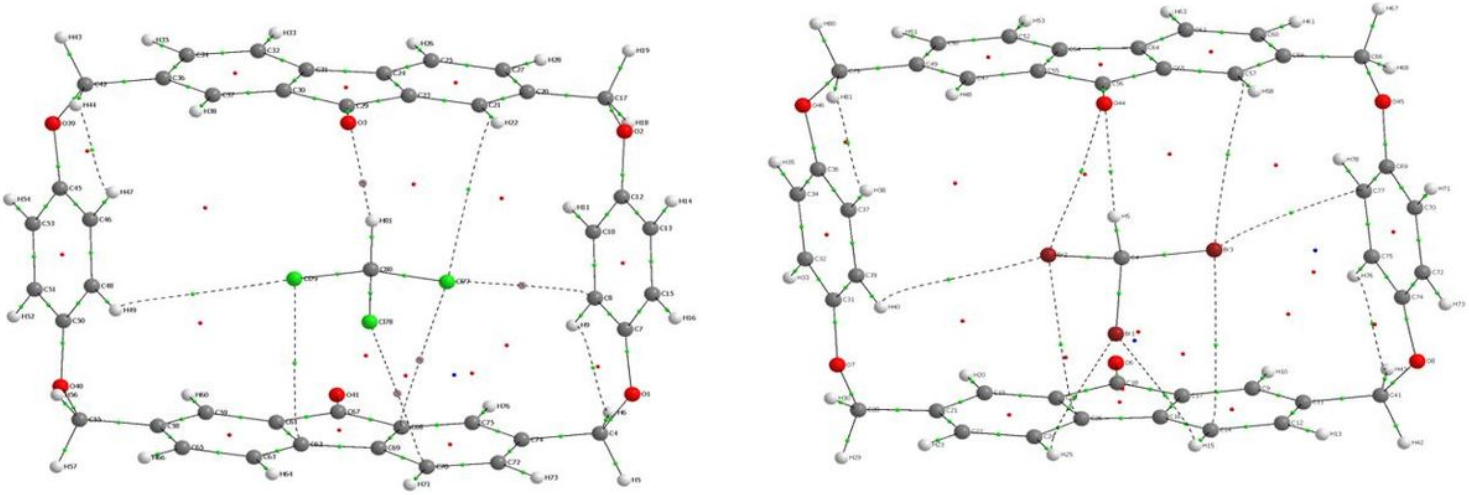

Figure 3

Interactions between fluorenonophane and haloform molecules according to the results of the AIM analysis.

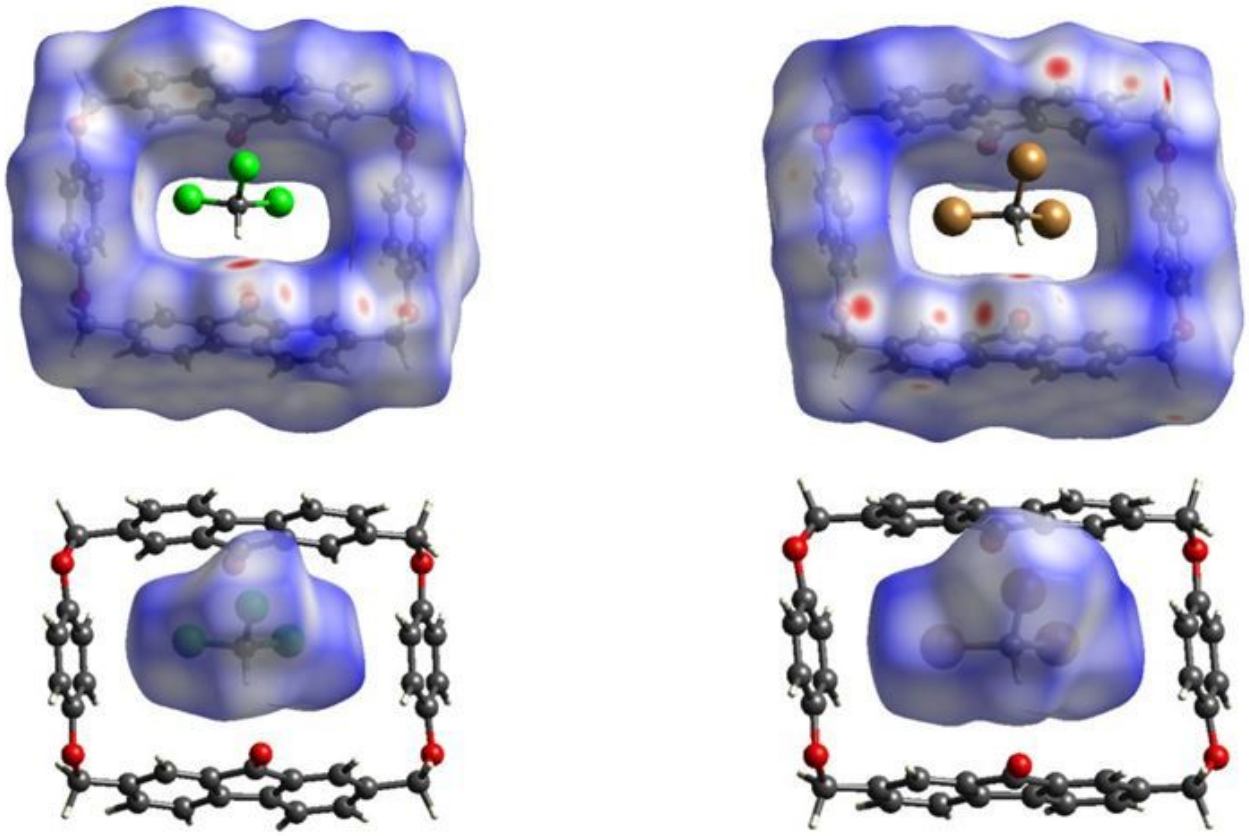

Figure 4

Hirshfeld surfaces with mapped dnorm property projected and transparency to show the conformation of the molecules for the complex 3Cl (on the left) and 3Br (on the right).

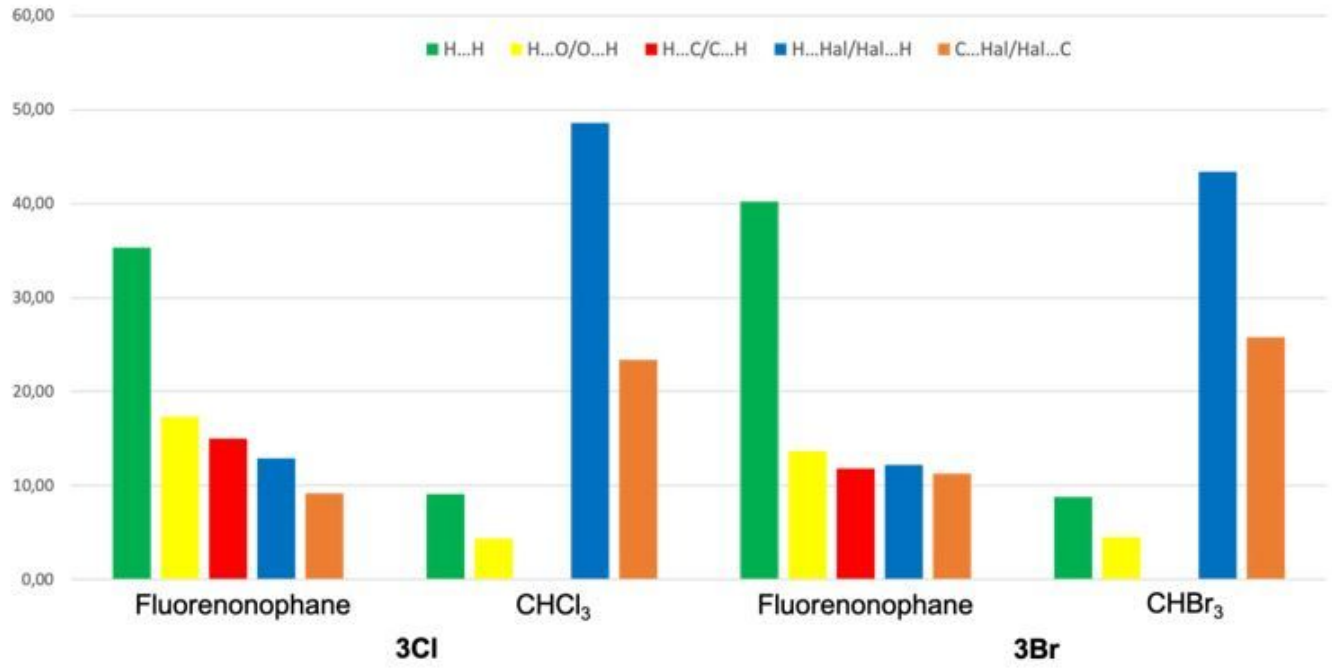

Figure 5

Relative contributions of the strongest intermolecular interactions (in %) to the total Hirshfeld surface for two polymorphic structures.

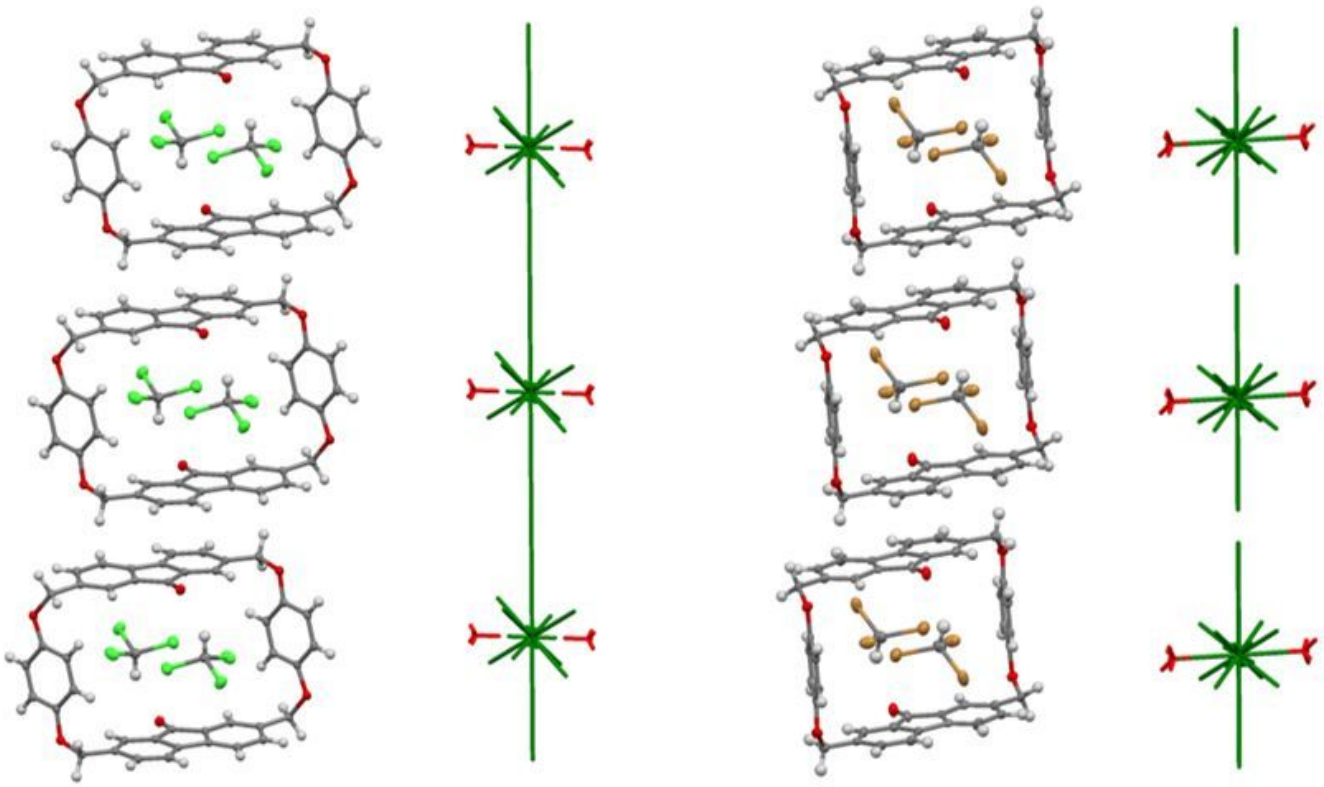

Figure 6

The main structural motif in the crystals of 3Cl (on the left) and 3Br (on the right) presented in terms of molecules and energy-vector diagrams. The EVDs of fluorenonophane are colored green while the EVDs of haloform molecules are colored red.

Supplementary Files

This is a list of supplementary files associated with this preprint. Click to download.

- ga.jpg
- ESI.docx
- S1.jpg